

Constraining bright optical counterparts of Fast Radio Bursts

Consuelo Núñez¹, Nicolas Tejos¹, Giuliano Pignata², Charles D. Kilpatrick³, J. Xavier Prochaska^{4,5}, Kasper E. Heintz^{6,7,8}, Keith W. Bannister⁹, S. Bhandari⁹, Cherie K. Day^{10,9}, A. T. Deller¹⁰, Chris Flynn^{10,11}, Elizabeth K. Mahony⁹, Diego Majewski⁴, Lachlan Marnoch^{12,9,13}, Hao Qiu¹⁴, Stuart D. Ryder^{12,13}, Ryan M. Shannon¹⁰

¹ Instituto de Física, Pontificia Universidad Católica de Valparaíso, Casilla 4059, Valparaíso, Chile
e-mail: consuelo.nunez.p@mail.pucv.cl; nicolas.tejos@pucv.cl

² Departamento de Ciencias Físicas, Universidad Andres Bello, Avda. República 252, Santiago, Chile

³ Center for Interdisciplinary Exploration and Research in Astrophysics (CIERA) and Department of Physics and Astronomy, Northwestern University, Evanston, IL 60208, USA

⁴ University of California Observatories-Lick Observatory, University of California, 1156 High Street, Santa Cruz, CA95064, USA

⁵ Kavli Institute for the Physics and Mathematics of the Universe (WIP), 5-1-5 Kashiwanoha, Kashiwa, 277-8583, Japan

⁶ Centre for Astrophysics and Cosmology, Science Institute, University of Iceland, Dunhagi 5, 107 Reykjavík, Iceland

⁷ Cosmic Dawn Center (DAWN), Denmark

⁸ Niels Bohr Institute, University of Copenhagen, Jagtvej 128, 2200 Copenhagen N, Denmark

⁹ Australia Telescope National Facility, CSIRO Astronomy and Space Science, PO Box 76, Epping, NSW 1710, Australia

¹⁰ Centre for Astrophysics and Supercomputing, Swinburne University of Technology, Hawthorn, VIC 3122, Australia

¹¹ ARC Centre of Excellence for Gravitational Wave Discovery (OzGrav), Australia

¹² Department of Physics and Astronomy, Macquarie University, NSW 2109, Australia

¹³ Astronomy, Astrophysics and Astrophotonics Research Centre, Macquarie University, Sydney, NSW 2109, Australia

¹⁴ Sydney Institute for Astronomy, School of Physics, University of Sydney, NSW 2006, Australia

February 12, 2022

ABSTRACT

Context. Fast Radio Bursts (FRBs) are extremely energetic pulses of millisecond duration and unknown origin. In order to understand the phenomenon that emits these pulses, targeted and untargeted searches have been performed for multi-wavelength counterparts, including the optical.

Aims. The objective of this work is to search for optical transients at the position of 8 well-localized FRBs, after the arrival of the burst on different time-scales (typically at one day, several months, and one year after FRB detection) in order to compare with known transient optical light curves.

Methods. We used the Las Cumbres Observatory Global Telescope Network (LCOGT), which allows us to promptly take images owing to its network of twenty-three telescopes working around the world. We used a template subtraction technique on all the images we collected at different epochs. We have divided the subtractions into two groups, in one group we use the image of the last epoch as a template and in the other group we use the image of the first epoch as a template. We have searched for bright optical transients at the localizations of the FRBs ($< 1''$) in the template subtracted images.

Results. We have found no optical transients, so we have set limiting magnitudes of optical counterparts. Typical limiting magnitudes in apparent (absolute) magnitudes for our LCOGT data are ~ 22 (-19) mag in the r -band. We have compared our limiting magnitudes with light curves of superluminous supernovae (SLSNe), type Ia supernovae (SNe), supernovae associated with gamma-ray bursts (GRB SNe), a kilonova, and tidal disruption events (TDEs).

Conclusions. We rule out that FRBs are associated with SLSN at a confidence of $\sim 99.9\%$. We can also rule out the brightest sub-types of type Ia SNe, GRB SNe and TDEs (under some conditions) at similar confidence, though we cannot exclude scenarios where FRBs are associated with the faintest sub-type of each of these transient classes.

Key words. fast radio burst – supernovae: general – techniques: photometric

1. Introduction

Fast Radio Bursts (FRBs) are extremely energetic radio frequency pulses that last for milliseconds or less (see e.g. Cordes & Chatterjee 2019, for a review). The dispersion measure (DM) of the FRBs is greater than the expected contribution of the Milky Way (e.g. Petroff et al. 2016), which gives us a clue about its extragalactic nature. These signals come from all directions in the sky and it is estimated that there are at least $\sim 1.7^{+1.5}_{-0.9} \times 10^3$

FRBs $\text{sky}^{-1} \text{day}^{-1}$ above $\sim 2 \text{Jy ms}$ (Bhandari et al. 2018a, see also Thornton et al. 2013).

Thus far, approximately one hundred of FRBs have been reported (Petroff et al. 2016; CHIME/FRB Collaboration et al. 2018; Heintz et al. 2020), but only a dozen of them are very well localized to sub-arcsecond precision (Chatterjee et al. 2017; Bhandari et al. 2020; Marcote et al. 2020). Thus, it has been possible to identify their host galaxies and redshifts, which confirms that they come from extragalactic sources. Most of these localizations, including those involved in this paper, have been detected by the Australian SKA Pathfinder (ASKAP) telescope (Johnston et al. 2008).

The first FRB was discovered in 2007 by Lorimer et al. (2007), and since then, the physical phenomenon that gives rise

Table 1. Observations summary

Field	Date	Site ^a	Seeing (")	Moon illumination	Background noise RMS (counts)
FRB180924	2019/05/31	SSO	2.0	15%	4.0
	2020/06/29	SSO	1.6	53%	3.9
FRB181112	2019/05/31	SSO	1.5	15%	4.5
	2020/06/29	SSO	3.5	53%	4.4
FRB190102	2019/05/31	SSO	2.3	15%	4.4
	2020/06/29	SSO	2.0	53%	4.3
FRB190608	2019/06/09	SAAO	2.2	35%	4.6
	2019/08/08	SSO	2.2	48%	4.8
	2020/06/29	SSO	3.3	53%	4.7
FRB190611	2019/06/11	SSO	1.9	54%	4.6
	2019/08/08	SSO	2.4	48%	4.7
	2020/06/29	SSO	3.4	53%	4.9
FRB190711	2019/07/11	SAAO	2.3	66%	4.3
	2019/08/08	CTIO	2.3	54%	6.7
	2020/06/29	SSO	1.8	53%	4.1
FRB190714	2019/07/14	SAAO	1.7	91%	8.8
	2019/08/08	CTIO	3.5	54%	13.1
	2020/06/30	SSO	1.6	53%	12.2
FRB191001	2019/10/05	SAAO	2.1	42%	4.5
	2019/11/26	CTIO	2.3	0%	4.9
	2020/06/29	SSO	3.4	53%	3.9

Notes. ^(a) SSO: Siding Spring Observatory, SAAO: South African Astronomical Observatory, CTIO: Cerro Tololo Inter-American Observatory.

to these bursts has been searched for. Many theories have been proposed about possible progenitors, the most popular involving core-collapse supernova (CCSN), superluminous supernova (SLSN)/long GRB, compact-object mergers like neutron star (NS), white dwarf (WD) or black holes (BH) mergers, magnetars and pulsars, and even superconducting cosmic strings (see e.g. Platts et al. 2019; Chatterjee 2020, for compilations). The recent detection of an intense radio burst within the Milky Way from the magnetar SGR 1935+2154 hints that at least the population of repeating FRBs could originate from magnetars (CHIME/FRB Collaboration et al. 2020; Bochenek et al. 2020; Margalit et al. 2020).

To understand more about the origin of FRBs, counterparts at different wavelengths have been sought, e.g. in optical range (Hardy et al. 2017; Tominaga et al. 2018; Marnoch et al. 2020; Kilpatrick et al. 2021), X-rays (Petroff et al. 2015; Scholz et al. 2016; Pilia et al. 2020; Tavani et al. 2020; Scholz et al. 2020) and Gamma rays (Yamasaki et al. 2016; Cunningham et al. 2019; Guidorzi et al. 2019, 2020). However, most of these searches have been reactive; that is, first the FRB is detected in the radio and then observations are triggered at the different wavelengths (Andreoni et al. 2020; Sun et al. 2021). This leads to a considerable time delay for these multi-wavelength follow-up observations.

In Marnoch et al. (2020) the first 3 FRBs well localized by ASKAP have been used to search for supernova-like transient optical counterparts with the Very Large Telescope (VLT). They triggered one image between 10 – 46 days after the burst detection and one image between 233 – 333 days later, in order to subtract them. They found no optical counterpart, so they put limits on the brightness of a potential transient. With a Monte Carlo approximation, they modeled light curves of different types of supernovae (SNe), concluding that Type Ia SNe and IIn SNe are unlikely to be associated with all non-repeating FRBs.

Recently in Kilpatrick et al. (2021) an optical follow-up of FRB180916 was made on 30 second timescales (with a time de-

lay of seconds to minutes), with the Apache Point Observatory (APO) in order to constrain the presence of optical emission contemporaneous with a radio burst. The repeating FRB180916 has a well established period of ~ 16.3 days, which has made possible a coordination of observations with the Canadian Hydrogen Intensity Mapping Experiment (CHIME), in the radio. CHIME has detected a radio pulse, while APO has not detected an optical transient within few seconds from the FRB time arrival. Also they ruled out models of a synchrotron maser from repeating magnetar flares where the burst energy was $> 10^{44}$ erg and circumburst density was $> 10^4$ cm $^{-3}$.

In this work, we searched for optical transients using the Las Cumbres Observatory Global Telescope Network (LCOGT) (Brown et al. 2013) at the position of 8 well-localized FRBs detected by ASKAP (Bhandari et al. 2020; Heintz et al. 2020), with data from the day of arrival of the FRB, up to ~ 1 – 2 years later. We find no transients in our search, and thus we present limits on emission from classes of luminous optical transients.

Compared to previous optical follow up work, we have analyzed a sample of several FRBs, rather than a single event (Hardy et al. 2017; Tominaga et al. 2018; Kilpatrick et al. 2021). In addition, we set limits on days very close to the arrival of the bursts (Marnoch et al. 2020), and our limits extend ~ 1 year after the FRB emission.

Despite the modest aperture of our telescope network, we were able to explore some extreme possible optical transient scenarios, such as superluminous supernovae (SLSNe) and the brightest sub-types of type Ia supernovae (SNe Ia) and gamma-ray bursts (GRB SNe).

We have explored the extreme scenario of tidal disruption event (TDE). These occur in supermassive black hole neighborhoods (Komossa 2015), and it has been previously shown by well-localized host galaxies that FRBs do not come from galactic centers (e.g. Bhandari et al. 2020; Heintz et al. 2020). Based on light curves of TDEs we seek to reaffirm TDEs are not related to FRBs.

Our paper is structured as follows. In Section 2 we present our observation strategy and the data obtained with LCOGT. In Section 3 we search for optical transients and place limiting magnitudes based our observations. The results are presented in Section 4 and the conclusions are presented in Section 5.

2. Data

2.1. LCOGT images

We used data from Las Cumbres Observatory Global Telescope Network (LCOGT; Brown et al. 2013) for this analysis. LCOGT is a network of twenty-three telescopes at seven sites around the world. We used the 1-m telescopes with Sinistro cameras, which have field of view (FoV) of $26.5' \times 26.5'$ and pixel size of $0.389''$. Dates, sites, seeing, Moon illumination and background noise RMS of all observations are listed in Table 1. The images were automatically processed through the BANZAI pipeline (McCully et al. 2018) with latest calibration frames¹.

The typical limiting apparent magnitudes obtained with our LCOGT data are approximately 22 mag in *r*-band (see Section 3.3). Nevertheless, one great advantage of using LCOGT for transient follow up is that the network is composed by telescopes all around the world, which allowed us to obtain images of each FRB field promptly (< 1 day for most of the fields).

2.2. Observation Strategy

Our observation strategy is to manually take an initial ‘epoch’ of optical imaging (ideally as soon as the FRB is detected) and then subsequent epochs after the initial one for monitoring purposes (typically 30 – 60 days after the first epoch motivated by the expected peak delays of SNe). For each epoch we obtained a set of 10 images of 60 s in the *r*-band.

Most of the fields were followed-up with rapid-response, which means the first epoch could be taken within the first day after the FRB detection; however, the fields FRB180924, FRB181112 and FRB190102 have first epochs taken with much longer delays (~ 100 days). We still include them in the analysis as these can constrain longer timescale transients such as SLSN. Table 2 summarizes the time delays incurred in each epoch for our different fields.

In the first epochs of FRB190608, FRB190611, FRB190711 and FRB190714, the images were taken with a several arcmin position uncertainties ($\approx 20' \times 20'$) as given by the analysis from ASKAP based on incoherent sum data (e.g. Shannon et al. 2018). For their second and third epochs, we have triggered the observations centred on the much more accurate position ($\sim 1 - 2''$) as given by the subsequent coherent ASKAP analysis (Bannister et al. 2019).

From this dataset we can make multiple comparisons between different epochs in order to search for putative bright optical transients. If no transient is seen, we set limiting magnitudes (upper limits in fluxes).

3. Analysis

3.1. Co-addition and Photometry

We co-added the 10 images from each epoch using the SWarp software (Bertin 2010), centering on the FRB coordinates in each field, with an image resampling method LANCZOS4 and

subtracting the background from individual images before resampling.

In order to obtain the photometry of each FRB field, we used the software “Source Extraction and Photometry” (SEP) (Barbary 2018; Bertin & Arnouts 1996). We empirically calibrated the magnitude zero points, by performing a cross-match between the point sources in our fields and the SkyMapper Southern Survey star catalog (Onken et al. 2019). After subtracting the background estimated by SEP, we calculated fluxes of all point like sources in our FoV using a circular aperture of 8 pixels radius, that is $\sim 3''$. We did not correct for our fixed aperture, which we have estimated to be of the order of 5%. These fluxes are compared with the fluxes of the objects detected by SkyMapper within an angular separation of $2''$ and eliminating saturated bright stars from the analysis, from which we are able to calibrate the magnitudes of our objects in our fields.

3.2. Search for Transients

Optical transients were searched at the precise FRB coordinates for each field. Images of the different epochs in a given FRB field were subtracted using the “High Order Transform of PSF And Template Subtraction” software (Becker 2015). The convolution parameters used are the following: the template was convolved, we used kernel order 2, background order 1, and 10 stamps in the *x* and *y* dimensions.

We produced two sets of template subtracted images: in one group, we use the image of the last epoch of in a given field as “template”, and in the other group we use the image of the first epoch in a given field as a “template”. In both cases “template” refers to the image that is subtracted from the other. Figure 1 shows an example of these subtraction groups for FRB190608.

We then run SEP on the image difference with a circular aperture radius of $2 \times \text{FWHM}$ and detection threshold of 1.5σ , in order to look for possible bright optical transients at the position of the 8 individual FRBs. No bright optical transients were detected using this method, so we proceed to set limiting magnitudes.

3.3. Limiting Magnitudes

Since we did not find any optical transients in our data, we set limiting magnitudes in order to compare such limits with models of possible progenitors.

3.3.1. Adding Mock Transients

In order to estimate the limiting magnitudes, we injected artificial stars (point-like sources) of different apparent magnitudes at the position of the FRBs in each image, in this manner mocking an unresolved optical transient. We estimated the FWHM of each LCOGT image by taking the average from three well-defined stars in the FoV (reported in the fourth column of Table 1). The artificial star is represented as a 2D Gaussian flux distribution, modeled according to the FWHM of each image.

After adding the artificial star to an individual image, we template subtract it (either the first or last epoch; see Section 3.2). Then, we proceed with the same automatic detection described above (see Section 3.2) and record the resulting signal-to-noise (S/N) of the source recovered, calculated by dividing the recovered flux and its recovered flux error at the position of the mock transient (i.e. the position of the FRB). We repeat this pro-

¹ i.e. reduction level code: 91.

Table 2. FRB fields and epochs of observations

FRB	1 st epoch (days)	2 nd epoch (days)	3 rd epoch (days)	z	Distance Modulus ^a	Galactic Extinction ^b
FRB180924	249	645	-	0.3212	41.15	0.04
FRB181112	201	596	-	0.4755	42.16	0.05
FRB190102	150	545	-	0.2912	40.91	0.52
FRB190608	1.20	61.6	387	0.1177	38.72	0.11
FRB190611	1.49	59.5	385	0.3778	41.57	0.52
FRB190711	1.07	30.0	355	0.5220	42.41	0.32
FRB190714	1.47	26.7	353	0.2365	40.39	0.14
FRB191001	5.14	56.3	273	0.2340	40.37	0.07

Notes. ^(a) Using Λ CDM cosmological parameter from Hinshaw et al. (2013). ^(b) Galactic extinction, A_r , based on Schlafly & Finkbeiner (2011).

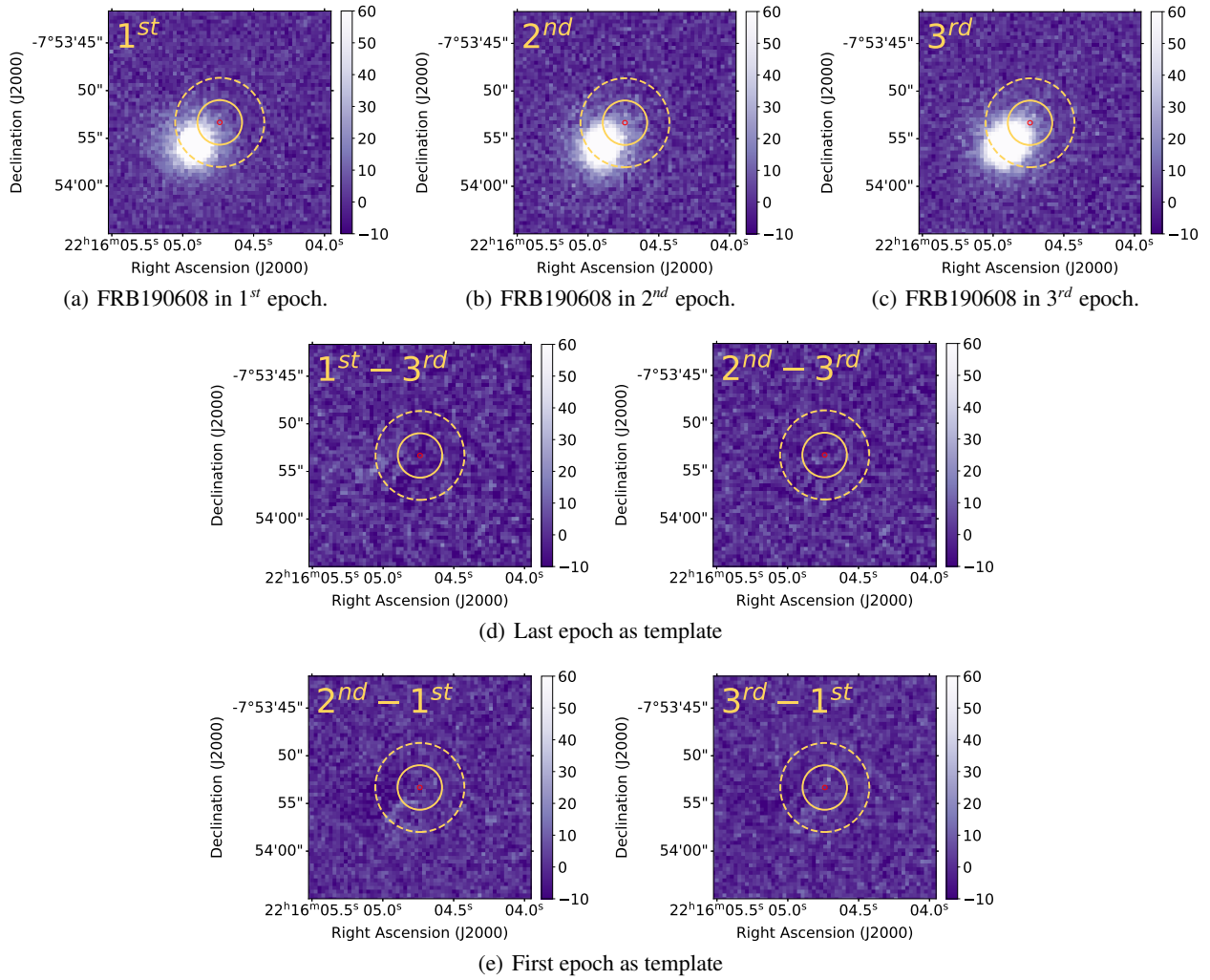


Fig. 1. Panels a), b) and c) correspond to the images of each epoch of the FRB190608 observations (three epochs in total for this FRB). Panels d) and e) show the difference images using the image of the last (3) and first (1) epoch as template, respectively. The solid (dashed) circle in all the panels represents the aperture radius of 1(2)×FWHM as reference, where FWHM = $\sim 2.3''$. Our photometric analysis uses an aperture radius of 2×FWHM to set the non-detection limiting magnitudes. The red ellipse represents the uncertainty in the FRB position.

cess for artificial stars of different apparent magnitudes, ranging from 17 to 25 mag and using 0.1 mag steps.

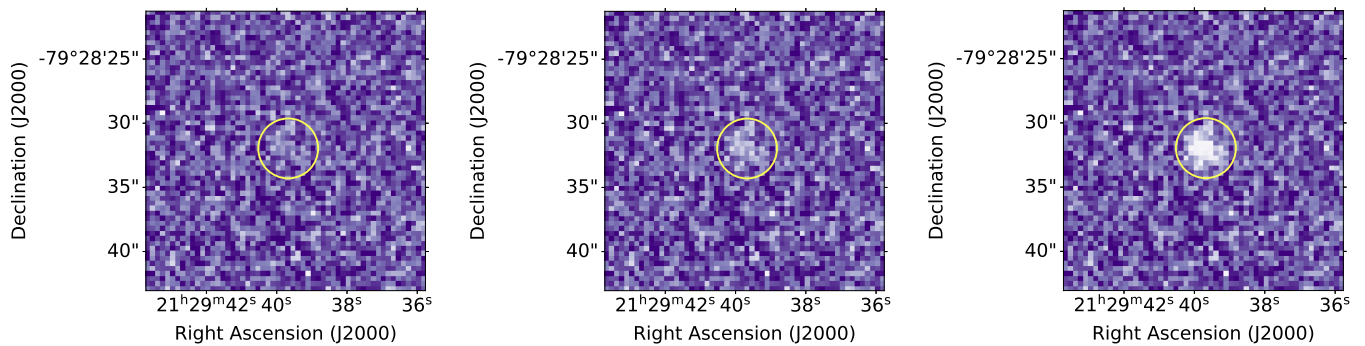
When the S/N of the recovered star is greater/lower than 3, we consider that a detection/non-detection (see Figure 2 for an example of this criteria). The recovered apparent magnitude is calculated through the flux, using a circular aperture radius of twice the FWHM. The limiting apparent magnitude in a given

epoch is set as the fainter recovered magnitude from the difference image with $S/N > 3$.

Since we have the redshift of the host galaxies of FRBs (i.e. the redshift of the FRB too), we obtained the absolute magnitudes using the Distance Modulus and taking into account Galactic extinctions (see Table 2). All the limiting apparent/absolute magnitudes for our different epochs are presented in Table 3.

Table 3. Limiting apparent/absolute magnitudes for each epoch.

FRB	Limiting Apparent/Absolute Magnitude				
	Last epoch as template		First epoch as template		
	1 st epoch (mag)	2 nd epoch (mag)	2 nd epoch (mag)	3 rd epoch (mag)	
FRB180924	22.5 / -18.7	-	21.9 / -19.3	-	
FRB181112	21.4 / -20.8	-	21.2 / -21.0	-	
FRB190102	21.8 / -19.6	-	22.3 / -19.1	-	
FRB190608	21.7 / -17.1	20.6 / -18.2	21.6 / -17.2	21.7 / -17.1	
FRB190611	21.1 / -21.0	21.4 / -20.7	21.9 / -20.2	22.0 / -20.1	
FRB190711	22.1 / -20.6	20.6 / -22.1	20.5 / -22.2	21.6 / -21.1	
FRB190714	21.0 / -19.5	20.4 / -20.1	20.8 / -19.7	22.1 / -18.4	
FRB191001	23.7 / -16.7	21.8 / -18.6	22.0 / -18.4	21.2 / -19.2	

**Fig. 2.** Example of difference images of two epochs of FRB190102 field, when one of them includes a mock point-like source injected of different magnitudes: non-detected source ($S/N < 3$; left panel), limiting magnitude ($S/N = 3$; center panel), and a well detected source ($S/N > 3$; right panel). The pale yellow circle indicates the position where we injected the mock star with an aperture radius of 1 FWHM as reference.

4. Results

Figure 3 shows the limiting absolute magnitudes of the 8 well localized FRBs studied here at different epochs, where the filled and empty triangles represent those that use the last and first epoch as template, respectively (see Section 3.2).

Although one may expect that the limits derived using the first or last epoch as template, should be the same, this is not always the case because the template subtraction process depends on the quality of both images involved in the process (e.g. background, PSF). Indeed, we observe a significant difference (although ≤ 1 mag) in the limits inferred for the second epoch of FRB190608, FRB190611 and FRB190714; these differences come mostly from the fact that the first and last epochs were observed with large differences in seeing conditions and/or moon-light illumination (see Table 1).

4.1. Comparison of limiting magnitudes with SN light curves

In the left panel to Figure 3 we include different light curves of bright optical transients in order to compare with the limits inferred above, assuming the FRB coincides with the triggering of the transient explosion. In particular, we focus the comparison with different types of bright supernovae (SNe), obtained from the “Open Supernova Catalog” (Guillochon et al. 2017). The catalog provides the light-curves in apparent magnitudes which we convert to absolute magnitudes adding the distance modulus (given the redshift of the SNe provided by the catalog), taking into account Galactic extinction, but not the intrinsic extinction of the host galaxy nor K -correction.

For this comparison we consider SLSN, GRB-SN and Type Ia SNe types. In order to have a representative range of SNe light-curves, we choose the brightest and the faintest of each type available in the catalog, for SLSN: SN2015bn (Nicholl et al. 2016) and SN2010md (De Cia et al. 2018); for GRB-SN: SN1998bw (McKenzie & Schaefer 1999) and SN2010bh (Olivares et al. 2012); and for type Ia SN: LSQ12gdj (Scalzo et al. 2014) and SN2009F (Pignata et al. 2009). The left panel in Figure 3 shows these ranges for the different types considered here. As reference, we have also added the light curve of a kilonova (Smartt et al. 2017). For plotting the light curves we have interpolated the datapoints of each type of SN, in order to obtain a smoothed curve.

Based on the comparison presented in Figure 3, we can rule out SLSNe as a possible progenitor model for all FRBs, since we have limiting magnitudes of 4 different FRBs under the light curve of the faintest SLSN catalogued. That is, if there had been an optical transient associated with SLSN, we would have seen it in our LCOGT data at a confidence of $\sim 99.9\%$ (see Section 4.2 for details). In contrast, for Type Ia and GRB SNe we can rule out only the bright end of the class, because normal and under-luminous Ia SNe lie below our detection limits. Similarly, our data is not deep enough to rule out a kilonova as possible progenitor of FRBs, as all our limits are above its light-curve.

4.2. Quantification for ruling out SLSNe

We have been setting the detection threshold as a constant value of 1.5σ in the difference image. This confidence interval gives us an 86.6% probability of finding the FRB between $x - 1.5\sigma < x < x + 1.5\sigma$, but since in our case they are limiting magnitudes,

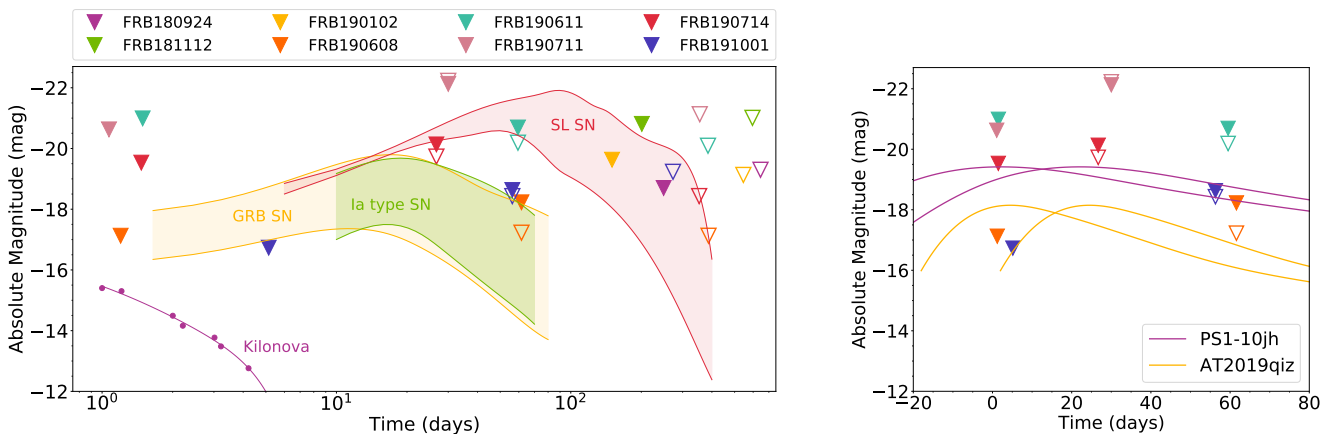


Fig. 3. Limiting absolute magnitudes at different epochs obtained for FRB positions (triangles) and light curves of different bright optical transients (color lines and regions). Filled (open) triangles correspond to those limits using last (first) epoch as template. In left panel: the red, yellow and green light curve bands represent SLSN, GRB SN, and type Ia SN respectively. Purple light curve is the kilonova. For the limiting magnitudes, the x-axis corresponds to the time since the FRB signal was received on Earth; for the light curves, the x-axis corresponds to the time since explosion. We emphasize that the x-axis is shown on a logarithmic scale and the y-axis is on the astronomical magnitude scale, such that brighter objects are at the top. In right panel: purple and yellow light curves represent two TDEs with luminosity peak in day 1 and day 21. Here the x-axis is presented in linear scale.

we need to integrate the probability distribution above $x + 1.5\sigma$, which results in 93.3%. That is, we have a 93.3% probability that the putative optical counterpart of the FRB is below its limiting magnitude, and thus a 6.7% probability that is above the reported limiting magnitude. Because we have multiple independent limits below the faintest SLSN we can put even more stringent limits by combining these probabilities.

Although by subtracting two images from two different epochs (i.e. by using the first or last epoch as template), we can obtain two limiting magnitudes for some epochs, it is important to note that these measurements are not independent. Thus, in order to combine limiting magnitudes we only take the most stringent one in a given epoch for a given FRB field that lie below the faintest SLSN curve, for a total of 4 independent ones.

Since we have 4 independent limiting magnitudes under the least bright light curve of SLSN, the probability of being above the 4 limiting magnitudes is $\sim 0.002\%$. In other words, we can rule out SLSN as a progenitor of all FRBs with a confidence level (c.l.) of $\sim 99.998\%$.

On a similar basis, we can rule out the brightest types of Type Ia SNe and GRB SNe at a similar confidence.

We note that these estimations are purely statistical in the sense that we assume no systematic uncertainties in the shape of the light curves. For instance, if we consider that the FRB arrival is -170 days or $+500$ days with respect to the SLSN explosion, in both cases we find only 2 upper limits instead of 4, corresponding to a 99.6% c.l. for ruling out an optical counterpart.

Finally, we also note that our previous estimates assume no extinction in the host galaxies. If we assume an extinction of 1 magnitude, we obtain 3 limiting magnitudes of FRBs under the representative faintest SLSN light curve instead of 4. However, if we consider the limiting magnitude associated to the first epoch of FRB191001 that is well below 1 mag of the extrapolation the SLSN to < 1 day earlier, our previous significance remains qualitatively similar.

4.3. Comparison of limiting magnitudes with TDE light curves

In the right panel of Figure 3 we have focused on the limiting magnitudes of the first days after the arrival of the FRB. We have

added light curves of two TDEs: AT2019qiz (Nicholl et al. 2020) and PS1-10jh (Gezari et al. 2015), obtained from the “Open TDE Catalog”.²

Since we do not know the exact time of the beginning of the event, we have plotted two possibilities for each TDE: (1) the FRB is emitted when the TDE reaches its peak luminosity; (2) the FRB is emitted 21 days before the TDE reaches its peak luminosity.

Taking into account possibility (1), we have 2 independent limiting magnitudes under the light curve of the weakest TDE. Following the quantification steps to discard SLSN in Section 4.2, we can rule out TDEs as possible progenitors of FRBs with $\sim 99.6\%$ c.l.. Now focusing on possibility (2), we can only rule out the brightest TDE with 4 independent limiting magnitudes under the light curve, that is, with $\sim 99.99\%$ c.l..

4.4. Dearth of prompt high-energy emission from GRB-SNe

We may put further constraints on the association of FRBs with other types of stellar transients, in particular GRB SNe, by quantifying the apparent lack of simultaneous high-energy prompt emission from the burst. Since the prompt GRB emission is highly beamed (Gehrels et al. 2009), only a fraction of FRB-emitting sources (in the case that γ -ray emission is directly associated with them) will have a detectable precursor GRB. This can be expressed approximately as $N_{\text{tot}} = N_{\text{visible}} / (1 - \cos(\theta_{\text{jet}}))$, such that for average jet opening angles $\theta_{\text{jet}} < 10^\circ$ (Frail et al. 2001; Bloom et al. 2003; Guetta & Piran 2005), only $\approx 1 - 2\%$ of GRBs will be detected. Convolved with the typical fraction of GRBs detectable by e.g. *Swift*/BAT at any given time (Lien et al. 2014), the probability of detecting a GRB associated with an FRB is $\lesssim 1\%$, assuming that the FRB emission is isotropic (or at least not similarly beamed as the GRB). We thus cannot rule out that prompt GRBs can be associated to FRBs given the still small number of well-localized FRBs.

² <http://TDE.space>

5. Conclusions

The search for progenitors of FRBs has become a challenge for the astronomical community over the last years. Unlike the works carried out by Hardy et al. (2017), Tominaga et al. (2018) and Kilpatrick et al. (2021), those looking for an optical counterpart associated only with a particular FRB, in this work we have a larger data sample, analyzing fields of view towards 8 different FRBs.

Although we have not found a transient that solves the mystery of the progenitors of FRBs, we have been able to rule out that SLSNe are one of them, at least over the timescales probed here (≈ -150 to $+500$ days) and for galaxy host extinctions $\lesssim 1$ magnitude.

SLSNe are rare explosions from poorly understood astrophysical phenomena associated with the ending lives of massive stars. They emit approximately 100 times more energy than typical SNe (Jerkstrand et al. 2020). With the data and the analysis obtained in this work, we can rule out the association of SLSN with FRBs with a confidence level of $\sim 99.99\%$. However, this does not rule out the possibility that the FRBs may come from a particular object, like a neutron star, which is surrounded by an extreme environment, such as an SLSN.

For Type Ia and GRB SNe, we can only rule out the most luminous ones of each class, as the faintest ones are too weak to be detected in our LCOGT data given our inferred limits and distances to the FRB hosts. Similarly, we cannot rule out a kilonova.

In contrast to the work done by Marnoch et al. (2020), we have data ~ 1 day after the arrival of the FRBs, which allowed us to rule out TDEs. These events occur when a star is torn apart by the tidal force of a supermassive black hole and emits a large amount of radiation. Given that most localized FRBs occur at projected positions that are inconsistent with being in the center of their host galaxies (Bhandari et al. 2018b; Heintz et al. 2020; Marcote et al. 2020; Mannings et al. 2020), one does not expect them to be associated with TDEs; our present results independently supports this conclusion on the basis of photometry.

Acknowledgements. This work makes use of observations from the Las Cumbres Observatory global telescope network (LCOGT), obtained as part of program programs CN2019A-39/CLN2019A-002, CN2019B-93/CLN2019B-001 and CN2020A-82/CLN2020A-001. C.N. and N.T. acknowledge support by FONDECYT grant 11191217. K.E.H. acknowledges support by a Postdoctoral Fellowship Grant (217690-051) from The Icelandic Research Fund. A.T.D. is the recipient of an ARC Future Fellowship (FT150100415). R.M.S. acknowledges support through ARC Future Fellowship FT190100155. L.M. acknowledges the receipt of an MQRES scholarship from Macquarie University. The Fast and Fortunate for FRB Follow-up team acknowledges support from NSF grants AST-1911140 and AST-1910471.

CHIME/FRB Collaboration, Andersen, B. C., Bandura, K. M., et al. 2020, *Nature*, 587, 54

Cordes, J. M. & Chatterjee, S. 2019, *ARA&A*, 57, 417

Cunningham, V., Cenko, S. B., Burns, E., et al. 2019, *ApJ*, 879, 40

De Cia, A., Gal-Yam, A., Rubin, A., et al. 2018, *ApJ*, 860, 100

Frail, D. A., Kulkarni, S. R., Sari, R., et al. 2001, *ApJ*, 562, L55

Gehrels, N., Ramirez-Ruiz, E., & Fox, D. B. 2009, *ARA&A*, 47, 567

Gezari, S., Chornock, R., Lawrence, A., et al. 2015, *ApJ*, 815, L5

Guetta, D. & Piran, T. 2005, *A&A*, 435, 421

Guidorzi, C., Marongiu, M., Martone, R., et al. 2019, *ApJ*, 882, 100

Guidorzi, C., Marongiu, M., Martone, R., et al. 2020, *A&A*, 637, A69

Guillochon, J., Parrent, J., Kelley, L. Z., & Margutti, R. 2017, *ApJ*, 835, 64

Hardy, L. K., Dhillon, V. S., Spitler, L. G., et al. 2017, *MNRAS*, 472, 2800

Heintz, K. E., Prochaska, J. X., Simha, S., et al. 2020, *ApJ*, 903, 152

Hinshaw, G., Larson, D., Komatsu, E., et al. 2013, *ApJS*, 208, 19

Jerkstrand, A., Maeda, K., & Kawabata, K. S. 2020, *Science*, 367, 415

Johnston, S., Taylor, R., Bailes, M., et al. 2008, *Experimental Astronomy*, 22, 151

Kilpatrick, C. D., Burchett, J. N., Jones, D. O., et al. 2021, *ApJ*, 907, L3

Komossa, S. 2015, *Journal of High Energy Astrophysics*, 7, 148

Lien, A., Sakamoto, T., Gehrels, N., et al. 2014, *ApJ*, 783, 24

Lorimer, D. R., Bailes, M., McLaughlin, M. A., Narkevic, D. J., & Crawford, F. 2007, *Science*, 318, 777

Mannings, A. G., Fong, W.-f., Simha, S., et al. 2020, *arXiv e-prints*, arXiv:2012.11617

Marcote, B., Nimmo, K., Hessels, J. W. T., et al. 2020, *Nature*, 577, 190

Margalit, B., Beniamini, P., Sridhar, N., & Metzger, B. D. 2020, *ApJ*, 899, L27

Marnoch, L., Ryder, S. D., Bannister, K. W., et al. 2020, *A&A*, 639, A119

McCully, C., Volgenau, N. H., Harbeck, D.-R., et al. 2018, in *Society of Photo-Optical Instrumentation Engineers (SPIE) Conference Series*, Vol. 10707, *Software and Cyberinfrastructure for Astronomy V*, 107070K

McKenzie, E. H. & Schaefer, B. E. 1999, *PASP*, 111, 964

Nicholl, M., Berger, E., Smartt, S. J., et al. 2016, *ApJ*, 826, 39

Nicholl, M., Wevers, T., Oates, S. R., et al. 2020, *MNRAS*, 499, 482

Olivares, F., Greiner, J., Schady, P., et al. 2012, *A&A*, 539, A76

Onken, C. A., Wolf, C., Bessell, M. S., et al. 2019, *PASA*, 36, e033

Petroff, E., Bailes, M., Barr, E. D., et al. 2015, *MNRAS*, 447, 246

Petroff, E., Barr, E. D., Jameson, A., et al. 2016, *PASA*, 33, e045

Pignata, G., Maza, J., Hamuy, M., et al. 2009, *Central Bureau Electronic Telegrams*, 1650, 1

Pilia, M., Burgay, M., Possenti, A., et al. 2020, *ApJ*, 896, L40

Platts, E., Weltman, A., Walters, A., et al. 2019, *Phys. Rep.*, 821, 1

Scalzo, R. A., Childress, M., Tucker, B., et al. 2014, *MNRAS*, 445, 30

Schlafly, E. F. & Finkbeiner, D. P. 2011, *ApJ*, 737, 103

Scholz, P., Cook, A., Cruces, M., et al. 2020, *ApJ*, 901, 165

Scholz, P., Spitler, L. G., Hessels, J. W. T., et al. 2016, *ApJ*, 833, 177

Shannon, R. M., Macquart, J. P., Bannister, K. W., et al. 2018, *Nature*, 562, 386

Smartt, S. J., Chen, T. W., Jerkstrand, A., et al. 2017, *Nature*, 551, 75

Sun, S., Yu, W., Yu, Y., & Mao, D. 2021, *ApJ*, 907, 25

Tavani, M., Casentini, C., Ursi, A., et al. 2020, *arXiv e-prints*, arXiv:2005.12164

Thornton, D., Stappers, B., Bailes, M., et al. 2013, *Science*, 341, 53

Tominaga, N., Niino, Y., Totani, T., et al. 2018, *PASJ*, 70, 103

Yamasaki, S., Totani, T., & Kawanaka, N. 2016, *MNRAS*, 460, 2875

References

Andreoni, I., Lu, W., Smith, R. M., et al. 2020, *ApJ*, 896, L2

Bannister, K. W., Deller, A. T., Phillips, C., et al. 2019, *Science*, 365, 565

Barbary, K. 2018, *SEP: Source Extraction and Photometry*

Becker, A. 2015, *HOTPANTS: High Order Transform of PSF ANd Template Subtraction*

Bertin, E. 2010, *SWarp: Resampling and Co-adding FITS Images Together*

Bertin, E. & Arnouts, S. 1996, *A&AS*, 117, 393

Bhandari, S., Keane, E. F., Barr, E. D., et al. 2018a, *MNRAS*, 475, 1427

Bhandari, S., Keane, E. F., Barr, E. D., et al. 2018b, *MNRAS*, 475, 1427

Bhandari, S., Sadler, E. M., Prochaska, J. X., et al. 2020, *ApJ*, 895, L37

Bloom, J. S., Frail, D. A., & Kulkarni, S. R. 2003, *ApJ*, 594, 674

Bochenek, C. D., Ravi, V., Belov, K. V., et al. 2020, *Nature*, 587, 59

Brown, T. M., Baliber, N., Bianco, F. B., et al. 2013, *PASP*, 125, 1031

Chatterjee, S. 2020, *arXiv e-prints*, arXiv:2012.10377

Chatterjee, S., Law, C. J., Wharton, R. S., et al. 2017, *Nature*, 541, 58

CHIME/FRB Collaboration, Amiri, M., Bandura, K., et al. 2018, *ApJ*, 863, 48